Discriminating brain activated area and predicting the stimuli performed using artificial neural network

Rafael do Espírito Santo

Pesquisador do Laboratório de Sistemas Integráveis –
EPUSP e Uninove; Pesquisador do Instituto Israelita
de Ensino e Pesquisa Albert Einstein (IIEP).;
Graduado em Engenharia Eletrônica
de Processos e Controle. (Universidade?)
Mestre em Controle de Processo e Doutor
em Engenharia Elétrica. (Universidade?).
São Paulo, SP – [Brasil]
rafaelid@uol.com.br

João Ricardo Sato

Instituto de Radiologia da Faculdade de Medicina da USP.
Pesquisador do Instituto de Radiologia
da Faculdade de Medicina da USP.
Doutor em Neuroimagens (USP) – Departamentos
Matemática e Estatística (IME).
São Paulo, SP – [Brasil]
jrsatobr@gmail.com

Maria G. Moraes Martin

Instituto de Radiologia da Faculdade de Medicina – USP;
Pesquisadora do Instituto de Radiologia
da Faculdade de Medicina da USP.
Doutor em Neuroimagens (USP) –
Faculdade de Medicina da USP.
São Paulo, SP – [Brasil]
mgmatim@cebinet.com.br

In this work, a Multilayer Perceptron implementation – MLP using functional Magnetic Resonance Imaging (fMRI) is used to infer stimuli performed. Sets of images of brain activation were generated by visual, auditory and finger tapping paradigms in 54 healthy volunteers. These images were used for training the MLP network in a leave-one-out manner in order to predict the paradigm that a subject performed by using other images, so far unseen by the MLP network. The aim in this paper is the exploring of the influence of the number of the Principal Component (PC) on the performance of the MLP in classifying fMRI paradigms. The classifier's performance was evaluated in terms of the *Sensitivity* and *Specificity*, *Prediction Accuracy* and the area A_z under the receiver operating characteristics (ROC) curve. From the ROC analysis, values of A_z up to 1 were obtained with 60 PCs in discriminating the visual paradigm from the auditory paradigm.

Key words: Activation. Classifier. FMRI. Neural networks. Paradigm.

Exacta, São Paulo, v. 5, n. 2, p. 311-320, jul./dez. 2007.

311

1   Introduction

Functional magnetic resonance imaging (fMRI) is a non-invasive imaging technique that can be effectively used to map different sensor, motor and cognitive functions to specific regions in the brain. It provides an open window onto the brain at work, exposing a relevant insight to the neural basis of the brain processes (HARDOON, 2005). By recording changes in cerebral blood flow, as a subject performs a mental task, fMRI shows which brain regions activate when a subject makes movements, hears or smells something, sees someone, thinks and so forth (HARDOON, 2005). The fMRI neuroimaging is considered by several researchers as a datum extremely rich in signal information and poorly characterized in terms of signal and noise structure (ROBINSON, 2004). Over the last few decades, fMRI developments and researches had got advances in interrelated fields such as machine learning, data mining, and statistics in order to enhance its capabilities to extract and characterize subtle features in data sets from a wide variety of scientific fields (ROBINSON, 2004). Among these developments, Artificial Neural Network (ANN), a sort of machine learning implementation, has been applied to a broad range of fMRI problems. One problem is: the stimulus inference based upon neuroimaging.

The aim in this work is to investigate the problem of inferring the neural stimulus performed by subjects using images of activation maps (converted into features vectors) that show patterns of brain activation induced by visual, auditory and finger tapping (left and right) paradigms. By using these images, a feedforward Multilayer Perceptron implementation (MLP) was trained to predict paradigm from other images so far unseen by the MLP network.

2   Functional magnetic resonance imaging

2.1 The BOLD effect

The fundamental physics used by the fMRI technique to produce functional and structural cerebral images is the contrast provided by the changes of the magnetic properties of the two states of hemoglobin: deoxyhemoglobin, the resulting molecule when some oxygen atoms are removed from the hemoglobin and oxyhemoglobin, Hemoglobin molecules fully saturated with oxygen (AMARO and BARKER, 2006; NAGY, et al, 2007). The first one is paramagnetic, so it is able to be attracted by a magnetic field. The second one is diamagnetic, namely, is slightly repelled by a magnetic field and does not retain the magnetic properties once the external field is removed (GIACOMANTONE, 2005; ERCC, 2007). One example of contrast imaging is the Blood Oxygen Level Dependent effect which the acroname is BOLD, in which the presence of oxyhemoglobin in a tissue produces a difference of susceptibility between the tissue and the neighboring area, that is, regions with high concentrations of oxyhemoglobin (tissue) provide brighter image than regions with low concentration – neighboring area (AMARO and BARKER, 2006). The temporal evolution of the BOLD effect is shown in figure 1.
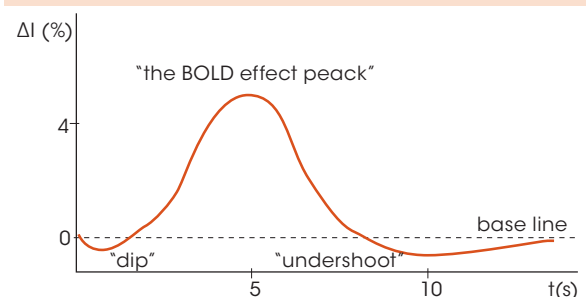

Figure 1: Hemodynamic response function from a hypothetical stimulus
Source: The authors.

2.2 Paradigm in fMRI

According to AMARO, E. and BARKER, G. J. (2006), paradigm in fMRI is the construction, temporal organization structure and behavioral predictions of cognitive tasks made by a subject during an fMRI experiment. Typical examples of fMRI paradigms are: visual, auditory and finger tapping paradigms.

2.3 fMRI scan

An fMRI scan measures the BOLD response at all the points in a three dimensional image or voxels (volume elements). A simple fMRI scan is able to collect three dimensional brain images (BOLD images) of the whole brain with approximately 10,000 to 15,000 voxels every 1-3s (MITCHELL et al, 2004; AMARO and BARKER, 2006). These BOLD images are a result of series of cognitive tasks (paradigm) performed inside the scanner by a subject (AMARO and BARKER, 2006). They show brightness levels changes of certain cerebral areas, proportional to the underlining activities, associated to the BOLD effect. The area in which the brightness changes in response to a specific paradigm made can be identified using statistical analyses or pattern recognition techniques (AMARO and BARKER, 2006).

3   Pattern classification

Here, we summarize only the relevant concepts for MLP-based classification that are essential for describing its application to fMRI. A full MLP description can be found in Haikin (1999). A MLP is a kind of Artificial Neural Network (ANN), assembled with a group of processing units (neurons) that are interconnected with varying synaptic weights. MLPs can be applied to a lot of areas within biology and neuroscience (HAYKIN, 1999; PETERS et

al, 2001), including fMRI data (MCKEOWN, 1998; MISAKI and MIYAUCHI, 2006). The popularity of MLP is primarily a result of its apparent ability of taking decisions and making conclusions when it deals with complex problems, defined in "noisy environment", or when the information used in the learning process are not enough to conduct the training or when the network has to adapt its behavior due to the nature of information used in the training (HAYKIN, 1999). In neuroimaging, MLP has been applied in data classification and pattern recognition to facilitate the diagnosis of pathological anomalies (diseases) and investigate functional activities of the brain.

3.1 MLP Architecture

The type of MLP we have used in our studies consists of a three-layered unit. They have neurons with adjustable synaptic weights and bias. The first and the third are the input and output layers, respectively. Between them there is a layer of hidden neurons. Each input neuron is connected to each hidden neuron by synaptic weights. Similarly, each hidden neuron is connected to each output ones by another group of synaptic weights (PETERS et al, 2001).

Figure 1 shows a representative model of a MLP neural network. In this figure one can identify the following elements (HAYKIN, 1999):

- A set of synaptic weights connections: a signal x_j in input synapse j, connected to the neuron k, is multiplied by the weight synapse w_{kj};
- Input signals, weighted by the correspondently synaptic weights, are summed with other input signals on a linear combination fashion;
- An activation function that limits the amplitude of output signal. The activation func-

tion, $\varphi(.)$, defines the output neuron in terms of active signal level in its input and provide a nonlinear characteristic to the MLP. An example of activation function is (HAYKIN, 1999):

$$\varphi(v) = \frac{1}{1 + e^{av}}$$

Figure 2: MPL neural network model
Source: The authors.

The network output is the value of activation function for v linear combination summing of the input level. It can also present an external threshold θ_k, that is, an offset from the normal output.

From figure 2,

$$u_k = \sum_{j=1}^{p} w_{kj} x_j$$

and

$$y_k = \varphi(u_k - \theta_k)$$

in which the sequences $x_1, x_2, ..., x_p$ and $w_{k1}, w_{k2}, ..., w_{kp}$ are the input signals and synaptic weights, respectively.

3.2 Training method

The training of an ANN consists of carrying out the input layer with cases examples of the problem at hand. The problem is solved by training the network with these cases examples, because, as the network manipulates different situation of the problem, it learns how to decide toward them.

The training applied to an ANN (HAYKIN, 1999) can be supervised. The training is realized as a set of cases examples put in the input layer, the correspondently output is compared to a threshold of acceptance. If the output is as good as desired, then, a backpropagation procedure is done (HAYKIN, 1999), namely, the updating procedure begins in the output layer and goes back toward the input layer. The training comes to an end when the network output values, compared to the threshold, are acceptable. A good example of ANN normally trained with the backpropagation procedure in a supervised manner is the MLP neural network.

4 Experimental results

4.1 Database description

In order to generate the database used in this study, a typical fMRI experiment that provides three-dimensional images related to the human subject's brain activity was conducted in the Radiology Institute (InRAD) of the *Faculdade de Medicina da Universidade de São Paulo* (FMUSP), in São Paulo, Brazil. In this experiment, carried out by Maria da Graça Moraes Martin, MD PHD, fifty-four healthy volunteers participated in a block designed fMRI that generated sets of images that show patterns of brain activation induced by visual, auditory and finger tapping (left and right) paradigms. The images were acquired using BOLD imaging technique on a clinical GE Sigma LX 1,5T

(Milkwalkee, USA) with fast acquisition gradient echo-planar image (EPI) sequence. BOLD imaging used 24 slices thickness/gap = 5/0.5mm from the cerebral cortex to the vertex, oriented according to the AC-PC line, BOLD sequence, TR/TE = 2000/0.4 ms, FOV = 24 mm and FA = 90 degree.

After acquiring all the images, the result database included a total of 216 cases examples (54 cases per paradigm), with a feature vector of length 19968 (number of brain regions). These cases examples were extracted from 54 images with resolution 64x64x25 pixel, exposing distinct activation maps obtained using the XBAM software (BRAMMER, M.J.; BULLMORE, E.T.; SIMMONS, A. et al,1997), applying the general linear model and wavelet permutation approaches.

4.2 Stimuli and paradigms

All paradigms were conducted following a cyclic block design fashion (condition 1, condition 2, alternating with resting). The four conditions were presented in two different experiments: visual-auditory and finger tapping Left/Right.

During the visual-auditory experiment, subjects were exposed to a flicking black and white chessboard and words were vocalized, in a periodic out-of-phase stimulation sequence, alternating with resting state conditions (visual-rest cycle of 16 seconds, auditory-rest of 24 seconds). The chessboard was projected in a screen outside the scanner, but visualized by the voluntaries using a mirror from inside. The words were listened by the subjects using headphones adapted to magnetic resonance systems.

In the motor experiment, the participants were asked to perform paced finger tapping movements with left, right or both hands according to a visual clue. As in the visual-auditory experiments, the sequence of movements was performed in a periodic out-of-phase stimulation sequence, alter-

nating with resting state conditions (motion-rest cycle of 20 seconds for both conditions).

4.3 Dimensionality reduction

It is hard to classify high-dimensional fMRI volumes into visual, auditory and finger tapping (left and right) paradigm. The dimension of each 54 brain activated image (converted into a feature vector of length 19968) is 256x78 pixel. Therefore, a dimensionality reduction must be done for decreasing the computational effort normally required to discriminate data like these.

The PCA formulation was used as a dimensionality reduction method. This formulation can be applied in image patterns identification and low-loss images compression by reducing the number of dimensions, without much loss of information (HAYKIN, 1999).

The bases of PCA formulation is the representation of an image in terms of its components (eigenvectors). In this formulation, it is formed a feature vector, a matrix of vectors, with the eigenvectors in the columns: *feature_vector* = (eig_1, eig_2, eig_3, ... eig_n). Each eigenvector has an associated eigenvalue. The *highest* eigenvalue is the first principle component (PC) of the image. The smaller ones are the less significant components. The dimensionality reduction consists of choosing the less significant components to leave out the feature vector.

The resulting compressed image is the one which the feature vector has as many less significant components as possible, which means as many principal components as possible (SMITH, 2002). Therefore, the image compression rate can be quantified from the number of PC chosen, that is, the less is the amount of PC the more compressed is the final image. In our studies compressed images with 10 to 60 PC were obtained.

Table 1: Training parameters used during the training session

Training	Principal components			
	10	20	50	60
The amount of hidden neurons	200	200	200	200
The number of layers	3	3	3	3
Epoch[1]	250/300	230/300	220/300	220/300
mse[2]	0.09/0.01	0.09/0.01	0.08/0.01	0.08/0.01
Learning factor (η)	0.6	0.6	0.6	0.6
Momentum (α)	0.999	0.999	0.999	0.999

[1] The training epoch: rate between the means value found for all training cases and the maximum value.
[2] The means square error (mse): the rate between the maximum performance and the performance goal.
Source: The authors.

4.6 Pattern recognition

The pattern recognition step can be organized in two sessions:

- The training session;
- The test session.

4.6.1 Training session

During the training session, the MLP with a hidden layer of 200 neurons was trained with a set of 216 (54 image per paradigm) compressed images translated into compressed feature vector (CFV). All the training session were performed in a leave-one-out fashion as described in section 4.4. The value of the training parameters of the MLP network (learning factor, momentum, total number of hidden neurons, etc.) were exhaustively chosen until the best MLP performance was obtained. Table 1 shows training parameters for each value of PC.

4.6.2 Test session

In the test session, predictions of a particular paradigm are performed (or visual or auditory or finger tapping) as described in section 4.4.

4.6.2.1 Classifier performance

The classifier's performance was evaluated in terms of the ratio of the number of test volumes wrongly classified to the total of tested activation maps (the error rate), the *sensitivity* and the *specificity* in separating the underlining paradigms: visual from auditory and left finger tapping from right finger tapping and the area A_z under the ROC curve.

4.6.2.1.1 Prediction accuracy rate

A classical manner to evaluate the classifier's performance is the computation of the *prediction accuracy* (the ratio of the number of test CFV correctly classified to the total of tested CFV). The graphic shown in figure 3 plots the *prediction accuracy* associated with some values of PC (image compression rate).
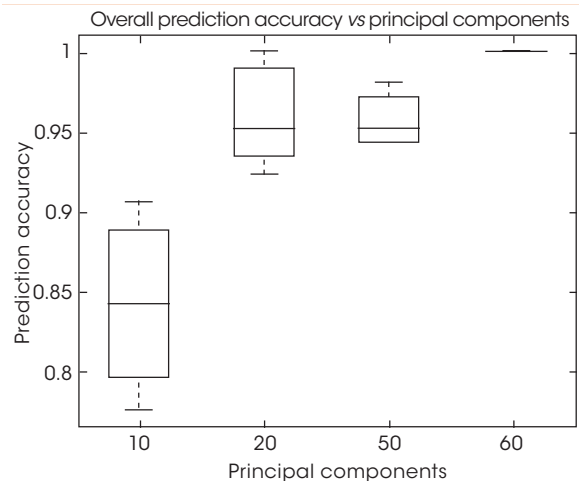

Figure 3: The dependence of prediction accuracy with the principal components
Source: The authors.

2.2.2.2.2 Sensitivity and specificity

Table 2 shows values of *sensitivity* (se) and *specificity* (sp) found during the test session related to the training set at hand, in two situations:

Sit_1 – The separation of visual paradigm from auditory paradigm.

Sit$_2$ – The separation of left finger tapping paradigm from right finger tapping paradigm.

The table also shows the influence of the number of principal components (PC) on the values of *sensitivity*, *specificity* and the elapsed time for each training session. The quantity of PC, as describe in section 4.5, establishes how compressed will be the final image after the application of the PCA formulation. According to this section, low values of PC produces images with high compression rate and high amount of PC produces an opposite situation. So it is interesting to demonstrate the influence (if any) of the image compression rate on the MLP performance.

Table 2: The influence of the principal components on the values of sensitivity (se) and specificity (sp)

Test with paradigm	Principal components							
	10		20		50		60	
	se	sp	se	sp	se	sp	se	sp
Visual vs. auditory[1]	0.98	0.85	1.00	0.93	0.98	0.94	1.0	1.00
Left finger tapping *vs.* right finger tapping[2]	0.84	0.98	0.96	0.94	0.96	0.98	1.0	1.00
Simulation time[3]	3h46min		5h16min		10h 05min		13h50min	

[1] se = probability of correctly predicting visual paradigm; sp = probability of correctly predicting auditory paradigm.

[2] se = probability of correctly predicting left finger tapping paradigm; sp = probability of correctly predicting right finger tapping paradigm.

[3] Time required for training the MLP network in leave-one-out fashion: The MLP code was written in MATLAB 7 language (R2006b) and run on a Pentium IV computer, with a speed of 3.0 GHz and RAM of 3 Gbytes.

Source: The authors.

4.6.2.1.3 The ROC curve

In this section, the classifier performance is evaluated in terms of the area A_z under the ROC curve (METZ, 1986; WOODS and BOWYER, 1997). For a specific value of PC, one ROC plots the ability of the MLP in separating visual para-

digm from auditory paradigm (figures 4 or 6 and another one plot the discrimination performed between right finger tapping and left finger tapping, figures 5 or 7).
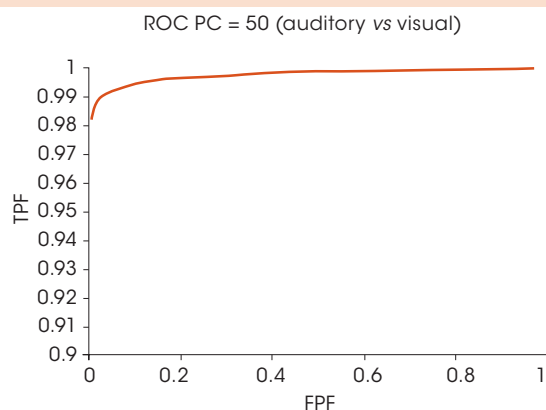

Figure 4: The ROC curve of the MLP classifier. TPF (True Positive Fraction) is the probability of correctly predicting auditory paradigm and FPF (False Positive Fraction) is the probability of incorrectly predicting auditory paradigm as visual paradigm. The area under curve (Az) is 0.998
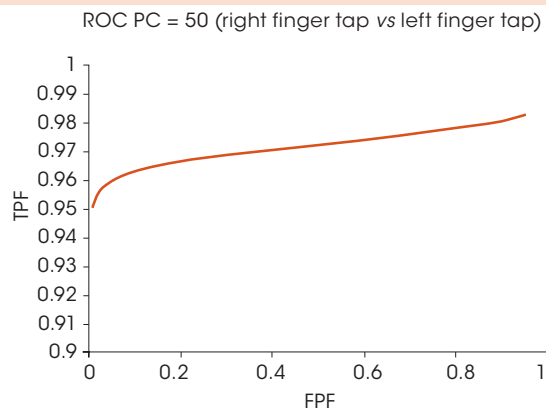
Source: The authors.

Figure 5: The ROC curve of the MLP classifier. TPF is the probability of correctly predicting right tapping paradigm and FPF is the probability of incorrectly predicting right tapping paradigm as left tapping paradigm. The area under curve (Az) is 0.972
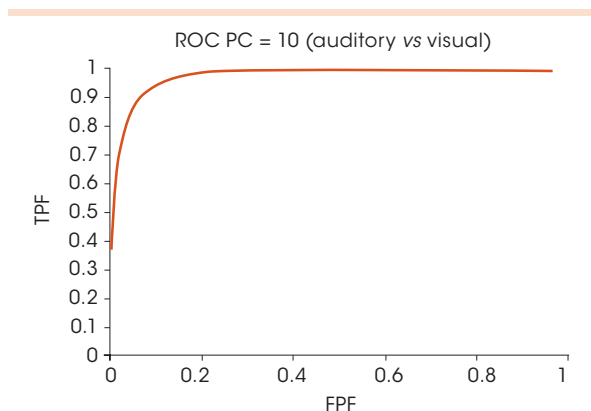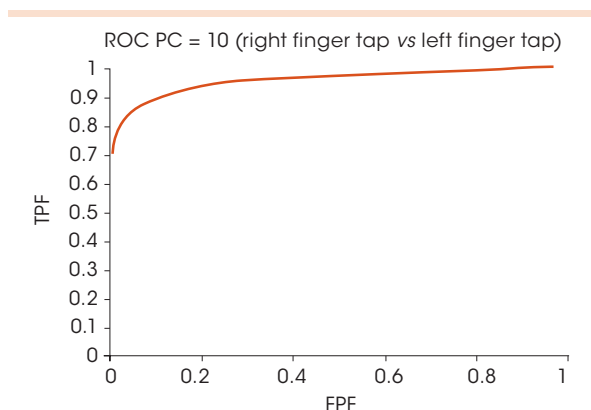
Source: The authors.

Figure 6: The ROC curve of the MLP classifier. TPF is the probability of correctly predicting auditory paradigm, and FPF is the probability of incorrectly predicting auditory paradigm as visual paradigm. The area under the curve (Az) is 0.976

Source: The authors.

Figure 7: The ROC curve of the MLP classifier. TPF is the probability of correctly predicting right tapping paradigm, and FPF is the probability of incorrectly predicting right tapping paradigm as left tapping paradigm. The area under the curve (Az) is 0.957

Source: The authors.

5. Discussion

5.1 Classifier performance in terms of prediction accuracy

The dependency of the MLP *prediction accuracy* with the number of PC is displayed in fig-

ure 3. Each PC indirectly expresses the compression rate of the images used for training the MLP network.

Section 4.5 briefly describes the dimensionality reduction provided by the PCA formulation. According to this section, the underlining formulation is an authentic low-loss image compression. The base of the data compression is the quantity of PC used. As mentioned in this section, the small is the amount of PC the higher is the image compression rate. However, compressed images with few PC should not be used to avoid loss of information and drops in classification's performance.

The graphic plotted in figure 8 confirms these arguments. As it can be seen, the median *prediction accuracy* of the MLP classifier assumes the values 1, 0.954, 0.953 and 0.843, respectively, as the classification is performed respectively with 60, 50, 20 and 10 PC.

5.2 Classifier performance in terms of sensitivity and specificity

In table 2, for visual and auditory paradigm discrimination, *sensitivity* is the probability of correctly predicting visual paradigm, and *specificity* is the probability of correctly predicting auditory paradigm. According to this table, the *sensitivity* and the *specificity* of the classifier are improved as the number of PC grows. This demonstrates that high image compression rate (low-PC) has a tendency to deteriorate the discrimination performance and a growing in PC (low image compression rate) produces relevant gains in overall performance. However, the performance in discriminating visual paradigm is slightly better (up to 7%, between 50 and 60 PC) than the ability in recognizing auditory paradigm.

For left and right finger tapping paradigm, *sensitivity* is the probability of correctly predicting left finger tapping paradigm and *specificity* is the probability of correctly predicting right finger

318

Exacta, São Paulo, v. 5, n. 2, p. 311-320, jul./dez. 2007.

tapping paradigm. The results shown in Table 2 are similar to those found with visual and auditory paradigm. In any case, an improvement in performance is observed as the amount of PC (decrease in image compression rate) increases from 10 to 60.

Additionally, in table 2 the simulation times are relevant information to perform a fast training session, with a desired compression rate (values of PC). As it can be seen on this table, for a particular prediction (high values of *sensitivity* and *specificity*), slow training session produces good classifier performance. So there must be a balance between training time and *prediction accuracy.*

5.3 Classifier performance in terms of the area under the ROC

Figures 5 to 8 display the performance of the classifier in discriminating the underlining paradigms in terms of the receiver operating characteristics (ROC) curve, which represents the variation of the true-positive fraction (TPF) versus the false-positive fraction (FPF) in pattern classification. The area under the ROC curve (A_z) may be used as a consolidated measure of classification accuracy or performance (METZ, 1986; WOODS and BOWYER, 1997).

In the ROC of figure 4, TPF is the probability of correctly predicting auditory paradigm, and FPF is the probability of incorrectly predicting auditory paradigm as visual paradigm. In the ROC of figure 5, on the other hand, TPF is the probability of correctly predicting right tapping paradigm and FPF is the probability of incorrectly predicting right tapping paradigm as left tapping paradigm. Comparing the values of A_z computed in these figures (0.998 and 0.972), regarding the previews arguments and the image compression rate (PC = 50), it is easy to conclude that the classifier performance in discriminating auditory paradigm from

visual is better than the performance in separating right tapping paradigm from left paradigm.

As for the case of PC 10, the meaning of TPF and FPF are the same of figures 6 and 7. The values of A_z however (0.976 and 0.957) are lower than the values with PC 50. This demonstrates the influence of image compression rate on the classifier performance. Comparing the values of A_z itself, one could get on the same conclusion: the classifier best performance is observed in the separation between auditory and visual paradigms.

6   Final considerations

In this study, it was demonstrated good accuracy of the MLP classifier in predicting (inferring) paradigms performed by subjects and the influence of the principal components (PC) on the inference performance as well. By using a MLP neural network, it is possible to infer what paradigm a subject performed from fMRI volumes, so far unseen by the MLP classifier. The desired inference accuracy can be foreseen from the amount of PC used for training the MLP. Our results show that training the MLP with high-PC produce better inference performance than training with low-PC even though there is a tendency of a too slow training session with high-PC. These results not only demonstrate the undeniable benefit of using MLP implementation in neuroimaging research, but also the possibility of saving training time by choosing the appropriated number of PC that produces the best inference performance.

To summarize, the novelty in this work was to demonstrate that it is possible to use a neural network implementation to infer the tasks performed by subjects. The bases of our approach deal with statistical parametric maps (translated into feature vector), PCA formulation and the

separation of them into groups of auditory, visual, left and right finger tapping paradigms.

References

AMARO, E. J.; BARKER, G. J. Study Design in fMRI: Basic principles. *Brain and Cognition*, v. 20, p. 220-232, 2006.

BRAMMER, M. J.; BULLMORE, E. T.; SIMMONS, A. et al. Generic brain activation mapping in fuctional magnetic resonance imaging: a nonparametric approach. *Magn Reson Imaging.* v. 15 p.763-770, 1997.

ERCC (2007) Diamagnetic, Paramagnetic, and Ferromagnetic Materials: Avaiable at <http://www.ndt-ed.org/EducationResources/CommunityCollege/MagParticle/Physics/MagneticMatls.htm>. Accessed in 08/10/2007.

GIACOMANTONE, J. O. *Ressonância Magnética Funcional com Filtragem pela Difusão Anisotrópica Robusta*. Dissertação de Mestrado. Escola Politécnica da Universidade de São Paulo, 2005.

HARDOON D, R. *One-class Machine Learning Approach for fMRI Analysis*. D R School of Electronics & Computer Science, University of Southampton, Southampton, UK L M Manevitz Department of Computer Science – University of Haifa. Haifa, Israel, 2005.

HAYKIN, S. *Neural Networks: A Comprehensive Foundation*. Prentice Hall, Upper Saddle River, NJ, 1999.

METZ, C. ROC methodology in radiologic imaging, *Investigative Radiology*, v. 21, p. 720-733. 1986.

MISAKI, M.; MIYAUCHI, S. Application of artificial neural network to fMRI regression analysis. *Neuroimage*, v. 29, p. 396-408. 2006.

MITCHELL, T.; HUTCHINSON, R.; NICULESCU, R. S.; PEREIRA, F. and WANG, X. "Learning to Decode Cognitive States from Brain Images". *Machine Learning*, v. 57, p.145-175, 2004.

NAGY, Z.; HUTTON, C.; NIKOLAUS, W.; DEICHMANN, R. "Functional Magnetic Resoanance Imaging of the Motor Network with 65ms Time Resolution". *Institute of Neurology, University College London*, 2007.

PETERS, B. O.; PFURTSCHELLER, G.; FLYVBJERG, H. Automatic differentiation of multichannel EEG signals. *IEEE Transaction on Biomedical Engineering*, v. 48. p.111-116, 2001.

ROBINSON, R. fMRI Beyond the Clinic: Will It Ever Be Ready for Prime Time? *PLoS Biol*. 2004 June; 2(6): e150. Published on-line, June 15.

SMITH L, I. A tutorial on Principal Components Analysis, 2002:

http://csnet.otago.ac.nz/cosc453/student_tutorials/principal_components.pdf. Accessed in 05/03/2007

WOODS, K.; BOWYER, K. W. Generating ROC curves for artificial neural networks, *IEEE Transactions on Medical Imaging*, v. 16, n. 3, p. 329-337, 1997.

320

Exacta, São Paulo, v. 5, n. 2, p. 311-320, jul./dez. 2007.